

Localized Tactile Feedback on a Transparent Surface Through Time-Reversal Wave Focusing

Charles Hudin, José Lozada and Vincent Hayward, *Fellow, IEEE*

Abstract—This article addresses the problem of producing independent tactile stimuli to multiple fingers exploring a transparent solid surface without the need to track their positions. To this end, wave time-reversal was applied to re-focus displacement impulses in time and in space at one or several locations in a thin glass plate. This result was achieved using ultrasonic bending waves produced by a set of lamellar piezoelectric actuators bonded at the periphery of the plate. Starting from first principles, the relations linking implementation parameters to the performance of the display are developed. The mechanical design of the display, signal processing and driving electronics are described. A set of engineering tradeoffs are made explicit and used for the design of a mock up device comprising a glass plate $148 \times 210 \times 0.5 \text{ mm}^3$. Tests indicate that a peak amplitude of $7 \text{ }\mu\text{m}$ confined to a 20 mm^2 region could be obtained for an average power consumption of 45 mW. Simultaneous focusing at several locations was successfully achieved. We showed that a lumped-mass model for the fingertip can effectively describe the effect of an actual fingertip load at the focus point. Lastly, we elucidated a likely stimulation mechanism that involves the transient decoupling of the finger skin from the plate surface. This phenomenon explains the observed tactile effect.

Index Terms—Tactile display, Time-reversal focusing, Plate vibration control, Piezoelectric actuated plate, Haptics

I. INTRODUCTION

THE tactile sense can be leveraged to enhance communication options with information devices such as graphical display panels, control consoles in cockpits, and other instances where the finger comes in contact with a surface for data entry, confirmation, and for interrogation.

Interesting interaction design options become available if the fingers can feel tactile signals that are collocated with the graphics [1]. Thus, the ability to remotize the transducers from the region of finger contact comes with the benefit that the touched surface may be made of a transparent material placed in front of a graphical display device. Such interactions would be greatly enhanced if several fingers could simultaneously feel different things on the same surface. This capability is not provided by any of the current surface tactile displays approaches since these

techniques cannot cause sensations that vary from region to region on a surface, without having to track the finger(s) position(s). Such a capability would enable the combination of graphical display with haptics, either via transparency or by projection, without the encumbrance of having to track finger(s) position. The same comments apply to instances of interaction with the feet instead of the fingers where the plate could be a solid floor [2]. In this article, we describe a technique that can provide these capabilities.

Displays based on matrices of actuators, each of which is dedicated to the stimulation of small region of skin, are ill-suited for integration with information devices, even if in some cases a significant measure of success was achieved [3]. In any case, distributed displays are bound to remain optically opaque and thus incompatible with overlaying on graphic displays, except, in some cases, via optical projection, which can be problematic because of occlusion.

Preserving optical transparency requires to remotize the actuators and to take advantage of the transmission of mechanical energy by waves or bulk displacement, with the possible exception of using the finger itself as an electrostatic actuator as in electro-vibration [4]–[7]. Bulk displacement of a solid for tactile stimulation has been used for half a century [8], is now commonly used by consumer electronic devices that include vibration motors, and has now been included in commercial vehicles [9]. More recently, standing wave ultrasonic vibrations have been employed to modulate friction between the finger and a transparent surface [10]–[14], with recent efforts to combined this approach with electrovibration [15].

From a physical point of view, the uniform distribution of mechanical energy in a vibrating solid with bulk displacement or with standing waves is energetically wasteful and also means that the signal displayed with these approaches can only vary in time. Of course, to obtain interactivity, the general idea is to correlate the temporal variations of mechanical energy with the finger movements in order to give the illusion that the surface properties vary in space. This illusion, however, breaks as soon as multiple fingers (or feet) are in contact with the surface.

Mechanical energy can also be transported in fluids. Gavrilov [16] demonstrated that focused ultrasound propagating in water could evoke tactile sensations. Shinoda and others took advantage of constructive and destructive interferences taking place between ultrasonic acoustic waves emanating from an array of transducers to produce a tactile stimulation that can be localized in space and in time in a

C. Hudin was with the CEA, LIST, Sensorial and Ambient Interfaces Laboratory, 91191, Gif-sur-Yvette Cedex, France. He is now with the Institut Langevin, ESPCI ParisTech, CNRS UMR 7587, F-75005 Paris, France (email: charles.hudin@espci.fr or charles.hudin@gmail.com)

J. Lozada was with the CEA, LIST, Sensorial and Ambient Interfaces Laboratory, 91191, Gif-sur-Yvette Cedex, France. He is now with the Mechatronics and Interactive Systems research centre, Universidad Tecnológica Indoamérica, Quito, Ecuador

V. Hayward is with Sorbonne Universités, UPMC Univ. Paris 06, UMR 7222, ISIR, F-75005, Paris, France

Manuscript received ...; revised ...

volume of air [17]–[20].

The aim of the present work is to apply the concept of time-reversed ultrasound waves propagating in thin plates with a view to realize localized tactile stimulation. Among the many types of mechanical waves that propagate in a solid, we considered the case of flexural waves since they induce out-of-plane displacements susceptible to be sensed tactually. In contrast with the case of free space, a thin plate is a bounded domain, i.e. a ‘cavity’, where waves reverberate. In such media, it can be shown that focusing cannot be achieved by driving the transducers with phased harmonic signals. Moreover, the dispersive nature of the flexural waves propagating in thin plates is another key difference with the propagation of waves in fluid-filled free-space domains. Dispersion means that wave propagation velocity depends on frequency. Intuitively, in a dispersive medium such as a plate, wave packets spread during propagation. Thus, delayed emission of harmonic flexural waves would not yield focusing at a single spot with a desired accuracy. The time-reversal technique, introduced by Fink [21], enables the focusing of any kind of waves in complex media and overcomes these two difficulties.

We investigated the outcomes of design tradeoffs for a multitouch, transparent tactile feedback interface based on re-focused waves by time-reversal. A mock-up device was built using 32 thin-plate actuators bonded to the sides of a 0.5 mm glass plate. Focusing was successfully achieved with this device and produced a 5 mm spot with a displacement amplitude of 7 μm for a power consumption of 45 mW. Focusing simultaneously in multiple points was also achieved and demonstrated the feasibility of displaying multitouch tactile stimulation. The mechanism underlying the tactile detection of the peak displacement produced at the focusing point was also explored since it is not straightforward to explain why a relatively small displacement can cause a rather powerful tactile effect.

II. TIME-REVERSAL FOCUSING

A. Principle

Wave time-reversal focusing is based on a symmetry principle according to which the evolution of physical quantities governed by differential equations involving only even-order temporal derivatives exhibit temporal symmetry. In other words, the solutions of these equations are invariant under the transformation of t into $-t$ [22]. Such is the case for the propagation of mechanical waves in any medium, as long as attenuation can be neglected. Fink showed that the initial state of a wave-field inside a bounded propagation domain can be reconstructed from temporal measurements of the wave field evolution at discrete locations. Partial reconstruction of a boundary condition with discrete transducers activated in a time-reversed fashion enables the reconstruction of a whole field at a given instant [21]. In particular, when the initial state is produced by a punctual impulsive source, the corresponding initial, and thus time reversed wave-field, is a spatial and temporal Dirac function. Time-reversal therefore enables the spatial

and temporal focusing of mechanical waves using a set of remote transducers in a reverberating, dispersive, and even scattering medium, as long as it is stationary. A review of the principle and applications of time-reversal focusing is given in [23].

B. Signal Processing

Time-reversal focusing of flexural waves in thin plates is achieved in two steps. In a first step, a set of Q transducers record the out-of-plane displacements produced by the propagation and reverberation of flexural waves resulting from an impulsive source located at a point, a , and during a period, T . The signal recorded by each transducer is the initial portion of the impulse response, $h_{aq}(t)$, between a source located at a and a transducer located at q . In a second step, these impulse responses are time-reversed to give $h_{aq}(T - t)$, and used as driving voltage for all the transducers. The re-emission leads to the re-focusing of the waves at point a and at time $t = T$ after the start of the re-emission.

This procedure is simple at first sight but raises significant difficulties in its practical implementation. A first issue is the need to produce sufficiently repeatable and calibrated mechanical ‘impulses’. A second issue is the need for a doubled electronics dedicated to reception in the learning phase and emission in the focusing phase. These issues can be circumvented by invoking another fundamental principle, that of reciprocity. According to the reciprocity principle, the inversion of the emission and reception points give an identical impulse response signal, that is, $h_{aq}(t) = h_{qa}(t)$. Thus, the response acquisition step can be achieved by sending a short electric impulse, $v_q(t) \approx \delta(t)$, to a given transducer, q , while recording the displacement, $u_a(t)$, at the point, a , where focusing is intended. A short, reproducible electrical impulse is much easier to achieve than a mechanical impulse. Thus, the transducers are actuators in the acquisition step as well as in the focusing step. There are many techniques available for displacement measurements including laser vibrometry, acceleration measurements, and others. A further practical improvement can be gained from a fundamental property of the Fourier transform. An impulse response, $h_{aq}(t)$, is the inverse Fourier transform of the transfer function $H_{aq}(\omega)$, a property widely used in system identification. To increase the input energy and therefore the signal-to-noise ratio, the impulsive input voltage is replaced by broadband signals such as white noise or chirped sines. In the frequency domain, the ratio of the measured displacement, $U_a(\omega)$, to the driving voltage, $V_q(\omega)$, gives the transfer function, $H_{aq} = \frac{U_a(\omega)}{V_q(\omega)}$, from which the impulse response can be obtained, $h_{aq}(t) = \text{TF}^{-1}[H_{aq}(\omega)]$, where TF^{-1} denotes the inverse Fourier transform. Impulse response with a satisfactory signal-to-noise ratio were experimentally achieved with a 200 ms swept sine.

The ability to focus at any position over the plate requires to measure or pre-calculate the impulse response between each point and the set of transducers. The interpolation of

impulse responses can be achieved by spatial oversampling when impulse response are measured over the surface with a uniform grid having a pitch equal to half of the shortest excited wavelength λ_{\min} . The total number of impulse responses to measure per transducer is thus equal to the plate surface area S divided by half of the minimum wavelength squared, that is $N_m = 4S/\lambda_{\min}^2$. Although more advanced techniques such as compressed sensing [24] or the method of fundamental solutions [25] allow for a reduction of the number of acquisition points, thousands of impulse responses typically need to be measured in order to be able to focus at any position on the plate.

C. Signal Generation

Another technique borrowed from signal processing ideas can further improve and simplify of the commissioning of time reversal wave focusing. The idea is to drive the actuators with a simplified, binary signal, $\text{sgn}[h_{aq}(T-t)]$. Derode et al. indeed demonstrated that preserving phase information not only maintains focusing quality, but also increases the displacement amplitude the focus point by a factor 2.4 for a same peak-to-peak driving voltage amplitude, V_{pp} [26]. The concomitant and additional benefit is the replacement of analog circuits by switching electronics. Furthermore, because the time reversal process is insensitive to DC components, a constant offset may be added to the signal in order to eliminate the need for bipolar amplification. The voltage, $v_{qa}(t)$, applied to a transducer, q , in order to focus at a point, a , reduces to,

$$v_{qa}(t) = \frac{1}{2}V_{pp} [1 + \text{sgn}(h_{aq}(T-t))],$$

which can be implemented using just two power transistors per channel driven by digital electronic circuits. Figure 1 summaries all these steps.

III. ENGINEERING TRADEOFFS

Surprisingly, the time-reversed emission of a single impulse response from a single actuator is sufficient to elicit the re-focusing phenomenon [27]. The characteristics of the focused wave-field and the resulting performances of a tactile display based on this approach thus depends on a variety of design parameters among which is the number of actuators. We now summarize the basic engineering tradeoffs that guide the design of a device.

A. Contrast

Contrast is defined to be the ratio of the amplitude reached at focused point a and time T to the quadratic average amplitude at any other location over the plate. It is related to the ratio of the energy density at the focus point and elsewhere. It is therefore a measure of focusing quality. The authors have previously shown that for a time-reversal experiment in a finite sized thin plate, the expression of the contrast ratio is given by [28],

$$C = \sqrt{BT_c} \sqrt{\frac{Q\tau [1 - \exp(-2T/\tau)]}{(Q+1)\tau [1 - \exp(-2T/\tau)] + T_c}}, \quad (1)$$

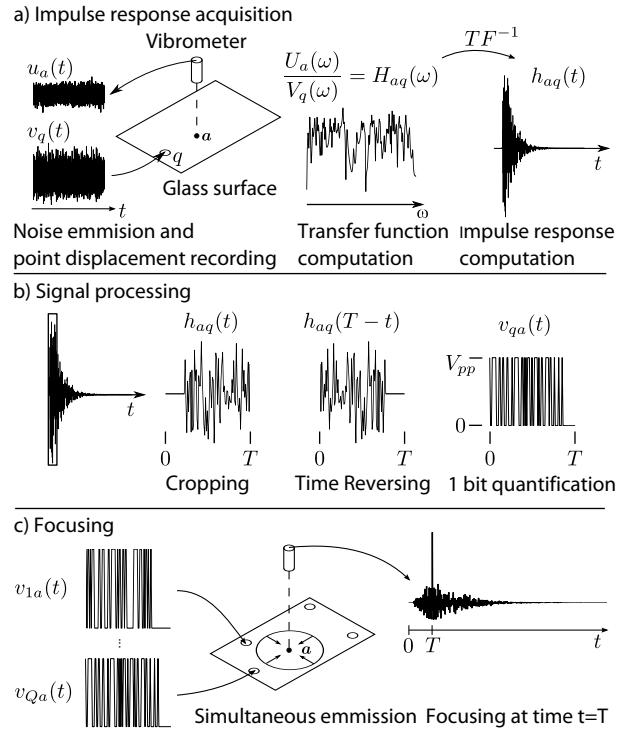


Fig. 1. Time-reversal procedure to focus waves at a point, a , using Q transducers. (i) The impulse response between a transducer at q and point at a is obtained by deconvolution of the measured displacement, $u_a(t)$, by the wide-band driving voltage $v_q(t)$ applied between the electrodes of the transducer. (ii) The T first seconds of the impulse response are cropped, quantified on one bit, offset and amplified. Steps (i) and (ii) are repeated for all transducers. The impulse responses are then simultaneously sent to all transducers in step (iii) to achieve the focusing at point a , T seconds after the start of emission.

where Q is the number of transducers, T is the duration of the focusing process, B is the bandwidth of the driving signals, τ the attenuation time constant of the vibrations in the plate, and T_c a time constant that depends on the plate dimensional and mechanical properties. This constant is given by,

$$T_c = \frac{\sqrt{3}S}{e} \sqrt{\frac{\rho(1-\nu^2)}{Y}}, \quad (2)$$

with S and e the plate surface area and thickness, and ρ , Y and ν the material density, Young's modulus and Poisson's ratio respectively. Equation (1) sets an upper bound, $C_{\max} = \sqrt{BT_c}$, on achievable contrast. Reaching high contrast values therefore requires to increase the signal bandwidth. When attenuation can be neglected, that is when $\tau \gg T$, maximum contrast is achieved when $QT \gg T_c$. A plate with low attenuation therefore makes it possible to increase the time-reversal duration, T , and thus to employ fewer actuators. Impulse responses however may drift significantly with temperature, thus making the time reversal of a set of pre-recorded impulse responses ineffective. It was thus shown that reducing the time-reversal duration T makes the focusing process less sensitive to environmental variations [28], [29].

B. Amplitude

Tactile detection thresholds are frequently given in terms of skin probe vibration displacement amplitude [30]. The ability to detect a stimulus produced by the described technique is therefore strongly dependent upon the amplitude of the displacement reached at focusing point and instant. In the case of time-reversal focusing in a reverberating medium, the amplitude, A , obeys [28],

$$A \propto Q\tau [1 - \exp(-2T/\tau)].$$

Increasing the number of sources, Q , or the duration of the time-reversal window, T , not only increases contrast but also leads to a larger peak displacement. Attenuation, however, ultimately limits the benefits of increasing T when $T \geq \tau$.

C. Resolution

Because of the finite bandwidth, B , of the drive signals, the focus point has a finite dimension and duration. The spatial resolution R_s , or -3 dB width, is defined as the size of the focusing spot at half maximum amplitude. This width is dictated by the diffraction limit and depends on the shortest wavelength λ_{\min} excited by the transducers such that [31],

$$R_s \simeq \frac{\lambda_{\min}}{2}. \quad (3)$$

Similarly, the temporal resolution, R_t , is the duration at half maximum amplitude of the focusing spot and depends on the highest frequency f_{\max} , or upper bound of the bandwidth B , excited by the transducers. Thus,

$$R_t \simeq \frac{1}{2f_{\max}}. \quad (4)$$

Because waves propagate in a plate, wave frequency and wavelength are related by the dispersion law given by [32, p.236],

$$\lambda_{\min}^2 = \pi \frac{e}{f_{\max}} \sqrt{\frac{Y}{3\rho(1-\nu^2)}}, \quad (5)$$

where ρ , Y and ν are the plate density, Young's modulus and Poisson's ratio respectively and e the plate thickness. Putting (3), (4), and (5) together gives a relationship between temporal and spatial resolution that reads,

$$\frac{R_s^2}{R_t} = \frac{\pi}{\sqrt{12}} e \sqrt{\frac{Y}{\rho(1-\nu^2)}}.$$

Spatial resolution, which limits under the spatial extend of a stimulus on the surface, is therefore entirely determined by the mechanical properties of the plate and by the highest frequency employed. Another consequence of this relationship is that the temporal and the spatial resolutions cannot be selected independently following an uncertainty principle. This result implies that the mechanical energy cannot be localized in space only. Spatial focusing with time-reversal in a bounded propagation domain is necessarily a transitory phenomenon.

D. Repetition

One approach to provide sustained stimulation is to repeat the focusing process in order to obtain a train of impulsive displacements. The repetition period, T_r , is limited by the attenuation of vibration in the medium since the instant of focusing concludes the convergence of a wave-front toward the focal point where it produces a peak displacement. Immediately after focusing, that is for time $t > T$, the wave-front diverges from the focus point, reverberates in the plate, and decays with a time constant τ . When the focusing process is repeated at a periodicity, T_r , that is smaller than the attenuation constant τ , decaying wave-fields resulting from previous impulses build-up, increasing the background average displacement over the plate. The focusing contrast is therefore sensitive to the repetition period. The effective contrast, \hat{C} , is governed by (see Appendix A),

$$\hat{C} = C \sqrt{1 - e^{-2T_r/\tau}},$$

where C is the contrast of an isolated impulse. Over 93% of the initial contrast is therefore preserved when $T_r \geq \tau$. Following (1), achieving a good contrast with few actuators limits the increase of the time-reversal window duration so that, $T \leq \tau$. On the other hand, a large attenuation constant precludes the repetition of the focusing process at a high rate. The plate should be designed be such that T , τ , and T_r have the same order of magnitude.

E. Energy balance

The effectiveness of the time-reversal approach for tactile stimulation depends on the amount of energy needed to achieve focusing at one point with a given amplitude, A , and spatial resolution, R_s . The evaluation (see Appendix B) of the total mechanical energy, E , contained in the plate at the focusing instant gives,

$$E = \frac{\pi^3}{18} \frac{Y}{1-\nu^2} e^3 \left(\frac{A}{R_s} \right)^2. \quad (6)$$

This energy corresponds to the energy transferred from the Q actuators to the plate during T seconds of emission. The average energy input per actuator is therefore $E_a = E/Q$ and the average power consumed by each actuator is $P_a = E/(QT)$. The plate thickness, e , is thus an important design parameter since the total energy grows proportionally to its cube.

IV. EXPERIMENTAL EVALUATION

A. Physical Setup

Mechanical design and actuators: These theoretical considerations were taken into account for the design of the mock-up device depicted in Fig. 2. This device is made of a borosilicate glass (Schott D263) plate with dimensions $L \times l = 210 \times 148 \text{ mm}^2$ and thickness $e = 0.5 \text{ mm}$ bonded to a rigid Polyoxymethylene frame by a 9 mm wide adhesive foam. The glass Young's modulus was $Y = 72.9 \text{ GPa}$, its Poisson's ratio $\nu = 0.208$, and its density

$\rho = 2510 \text{ kg}\cdot\text{m}^{-3}$. Inserting these values into (2) gave a plate characteristic time of $T_c = 19.5 \text{ ms}$. Impulse responses were measured following the method summarized in Fig. 1. Fitting a decaying exponential on these impulse responses gave the attenuation constant $\tau = 1 \text{ ms}$.

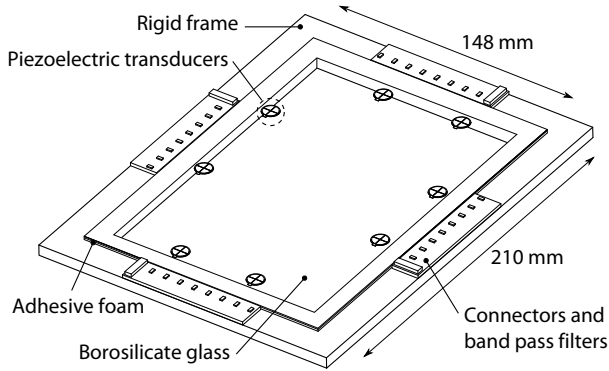


Fig. 2. Sketch of mock-up device.

The highest frequency was selected to be $f_{\max} = 70 \text{ kHz}$ in order to produce, according to (5), wavelengths as low as $\lambda_{\min} \simeq 10 \text{ mm}$ and hence to produce a focal spot with resolution $R_s = \lambda_{\min}/2 \simeq 5 \text{ mm}$. The impulse responses were high-pass filtered before the emission step to discard audible frequency components below 20 kHz. The bandwidth was therefore $B = 70 - 20 = 50 \text{ kHz}$.

Eight piezoelectric diaphragms (Muratta 7BB-12-9) were bonded with epoxy to the upper surface of the glass plate, at a distance $d \simeq 10 \text{ mm}$ from plate sides. Such actuators, when coupled to a thin plate, cannot produce wavelengths smaller than twice their dimension [33]. To produce wavelengths as low as 10 mm and thus to be able to reach the desired spatial resolution, the outer ring of each diaphragm was removed and a pattern of four electrodes was cut on top of each diaphragm, as depicted in Fig. 3. In this way, a total number of $Q = 8 \times 4 = 32$ actuators with dimension about 5 mm was obtained.

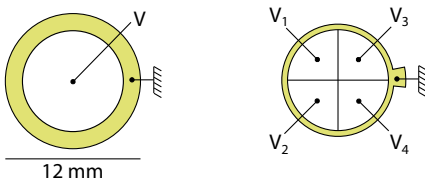


Fig. 3. Obtention of four transducers from the cutting of the top electrode and of a piezoelectric diaphragm (Muratta 7BB-12-9).

Driving electronics: A Field-Programmable Gate Array (FPGA) produced the 32 digital drive signals. An amplification stage, see Fig. 4 for one actuator, elevated the drive signal to provide a binary 0–60 V voltage to each actuator. The capacitance of piezoelectric actuators was $C_p = 2 \text{ nF}$. A resistor, $R_f = 2 \text{ k}\Omega$, and an inductor, $L_f = 6.8 \text{ mH}$, acted as a band pass filter in the bandwidth, B . The filter central frequency and -3 dB bandwidth were $f_0 = (1/2\pi)\sqrt{1/(L_f C_p)} = 43 \text{ kHz}$ and $\Delta_f = \sqrt{3}/(2\pi R_f C_p) = 69 \text{ kHz}$, respectively. Figure 5 shows

a picture of the mock-up device along the amplification circuit and the FPGA controller.

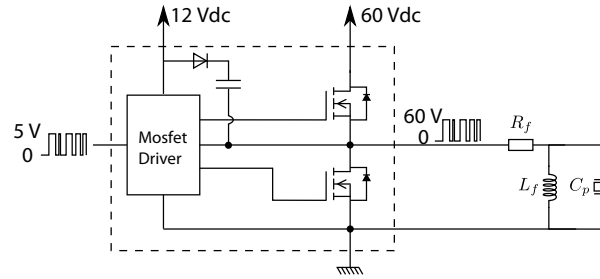


Fig. 4. Schematics of the amplification stage. Two field-effect transistors (DiodesZetex ZXMN10A08), mounted in push pull configuration and driven by a mosfet driver (Texas Instrument LM5104), amplify the digital signal produced by the FPGA controller from 5 V to 60 V. A resistor, R_f , and an inductor, L_f , form with the transducer capacitance, C_p , a RLC bandpass filter retaining only the 20-70 kHz frequency components.

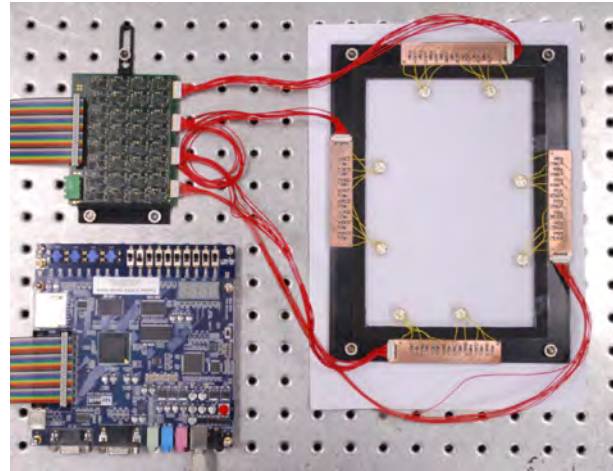


Fig. 5. Picture of the mock-up device (right) with the amplification stage (top left) and FPGA controller (bottom left).

B. Results

Single point focusing: To reach maximum contrast and maximize the amplitude the time-reversal window duration was set to $T = 2 \text{ ms}$. Focusing at the same position was repeated while a vibrometer (Polytec, OFV 534) scanned the surface by steps of 2 mm to measure the out-of-plane displacements over a $200 \times 148 \text{ mm}^2$ grid. The excellent repeatability of the focusing process combined with the synchronization of the vibrometer acquisitions with emissions enabled the reconstruction of the temporal evolution of the displacement over the surface. Snapshots of this evolution are shown in Fig. 6 (top panel) where a converging wave-front that giving birth to a focused spot at time $t = 2 \text{ ms}$ and then diverges and decays for $t > T$.

Figure 7 represents the pseudo three-dimensional displacement at focusing time showing the spatial spread of the produced displacement, relatively to the tactile surface. The measured focus spot amplitude is $A^{\text{meas}} = 7.68 \text{ }\mu\text{m}$. The measured spatial resolution was $R_s^{\text{meas}} = 5.2 \text{ mm}$ and

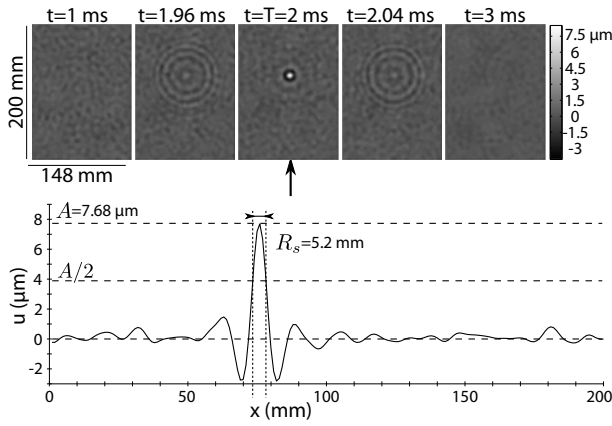


Fig. 6. Out-of-plane displacement of the plate measured during the focusing process (top). Waves produced by the transducers ($t = 1$ ms) form a converging wavefront ($t = 1.96$ ms) that gives birth to the focusing spot at time $T = 2$ ms. Focusing is followed by a diverging wavefront ($t = 2.04$ ms) that is reverberated and damped out ($t = 3$ ms). The displacement at focus time and position (bottom) reaches $A = 7.68 \mu\text{m}$ for a spatial resolution $R_s = 5.2$ mm.

agreed well with the resolution $\lambda_{\min}/2 \simeq 5$ mm expected from the theoretical considerations of the previous section. The measured contrast ratio, $C^{\text{meas}} = 29$, was, again, close to the theoretical value $C = 24$ obtained from (1).

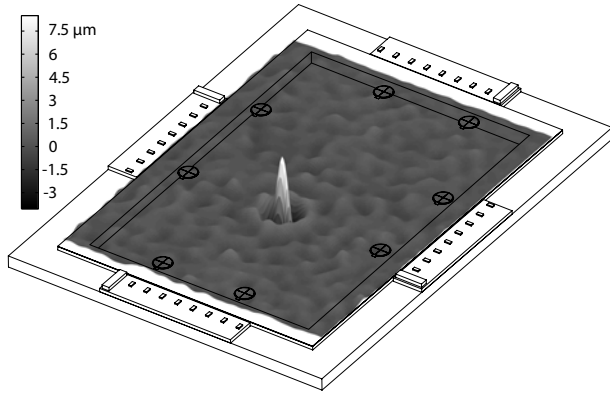


Fig. 7. Glass plate displacement measured at focus time (out-of-plane scale exaggerated for clarity).

The energy stored into the plate can be calculated from the measured out-of-plane displacement (see Appendix B). The evolution of the sum of potential and kinetic energy is shown in Fig. 8. The plot shows a steady build-up of mechanical energy until the end of the emission period at time $T = 2$ ms where the energy reaches its maximum, $E \simeq 90 \mu\text{J}$. The maximum corresponds, up to the energy dissipated during the first 2 ms, to the total energy spent by the actuators to achieve the focusing. The average power spent by all actuators is therefore $P = 90 \mu\text{J}/2 \text{ ms} = 45 \text{ mW}$. After focusing, the actuators no longer are energized and the total energy decays with time constant, 2τ . Inserting the values of the focused point amplitude and resolution, into (6) gives a theoretical value $E = 59 \mu\text{J}$ for the total mechanical energy spent, it is thus slightly underestimated by 34%. Expression (6) is therefore a valuable tool for the design of time-reversal based tactile

displays. As a practical point of comparison, the study in [34] reports that the consumption of a smartphone during web browsing is about 400 mW with screen backlight off and doubles with a full brightness backlight.

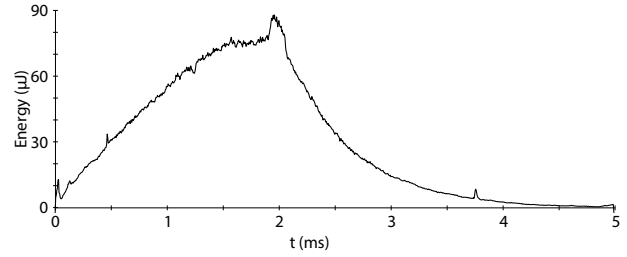


Fig. 8. Mechanical energy stored into the plate during focusing, calculated from the measured out-of-plane displacement. The energy increases between $t = 0$ and $t = 2$ ms due to the energy input from transducers. The maximum energy $E = 90 \mu\text{J}$ is reached at focus time $t = 2$ ms and then decreases exponentially owing to vibration natural attenuation.

Simultaneous focusing in four points: Provided that wave propagation in the plate can be considered to be linear, the wave field produced by N simultaneous mechanical impulses on the plate is the sum of the wave fields produced by each impulse alone. Focusing any shape at the plate surface requires to superimpose the impulse responses corresponding to each position weighted by the desired amplitude at the focal points. Multiple focalization can be illustrated by simultaneous focusing at four points distant by $L = 2R_s = 10$ mm. Four impulse responses with equal amplitude where summed *before* quantification since quantization is nonlinear transformation. Figure 9 shows the resulting displacement measured within a $40 \times 40 \text{ mm}^2$ area at focusing time, $t = 2$ ms. As anticipated, the spatial resolution $R_s = 5$ mm is not affected by multiple focalization. The amplitude $A = 2.9 \mu\text{m}$ reached at the four focal points is smaller than for a single point, following the principle of conservation of the energy injected in the system.

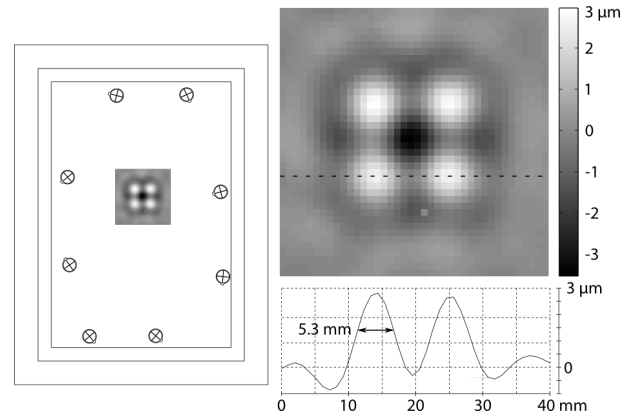


Fig. 9. Plate displacement measured at focus time while focusing simultaneously at four points. The amplitude reached at focus points $A = 2.9 \mu\text{m}$. The spatial resolution $R_s = 5.3$ mm is preserved.

The distribution of the learning points is arbitrary. Furthermore, when the responses are initially measured over a regular grid with a pitch equal to half the wavelength,

Fourier interpolation can be employed to reconstruct with no loss the impulse responses at intermediary positions. Focusing points on a regular grid is therefore a special case intended to demonstrate the ability of our technique to discriminate points distant by one wavelength. Focusing at points not aligned with the grid or displacing them continuously at the surface can also be performed with no added difficulties.

C. Discussion

These results demonstrate the feasibility of taking advantage of time-reversal focusing in a thin plate to produce a localized, tangible out-of-plane displacement concentrated in an area smaller than the contact area between a finger and a flat surface. The amplitude at the focal point is greater than tactile detection thresholds reported in literature and we found that the energy and power required to achieve such focusing are compatible with their use in mobile devices. Displaying stimuli at multiple locations can be achieved either by focusing alternatively on each point or by simultaneous focusing at multiple points. In the first case, the vibration attenuation constant, τ , has to be sufficiently small to allow for high repetition rates of impulses, while the second approach requires high contrast and more amplitude since the amplitude in each focal point decreases with their number. Another option is to mix these approaches.

V. FINGER INTERACTION

Until now, we have considered the case of an unloaded plate, free from finger contact. Touching the plate, however, locally increases the mechanical loading impedance and may scatters flexural waves. In particular, touching the plate at the focus point can be expected to decrease the amplitude of the re-focused displacement impulse. In this section, we develop a model able to predict these effects.

A. Model

The fingertip impedance was measured and modeled in the past in the quasi-static regime [35]–[39]. In the dynamic range, 0–1,000 Hz, a lumped element model of the fingertip impedance subjected to a shearing loads was recently identified [40]. These studies suggest the dominance of the inertial term in the high frequencies corresponding to a very short transitory impulse. Adopting a lumped inertial fingertip model, the peak displacement, \tilde{A} , of the plate loaded by the finger is related to the free plate peak displacement, A , (see Appendix C),

$$\tilde{A} = A \left[1 - \exp \left(-\frac{8R_s^2 \rho e}{\pi M} \right) \right], \quad (7)$$

where M is the finger lumped mass. For a given plate of density, ρ , and target resolution, R_s , a thicker plate increases the ratio \tilde{A}/A and thus desensitizes the peak displacement from contact. The finger attenuation follows a decreasing exponential relationship with plate thickness

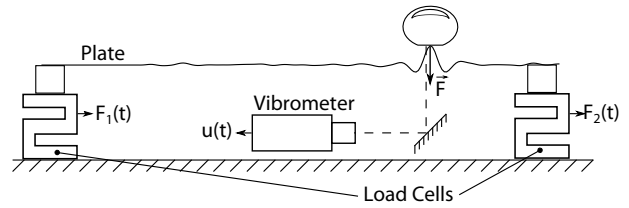


Fig. 10. Setup for the measurement of the peak displacement attenuation at focus point due to finger contact. The vibrometer laser beam was deflected by a mirror and reflected back on the bottom side of the plate. Two load cells measured the force exerted by a finger at focus point.

while the power consumption grows as a cubic power of thickness. Thus an appropriate value results from a balance between these two effects. Determining an appropriate thickness requires the knowledge of the fingertip equivalent mass, M , that is displaced at the instant of impact.

Spatial resolution, plate density and thickness being known quantities, rewriting (7) gives the apparent fingertip mass M ,

$$M = \frac{8}{\pi} \frac{R_s^2 \rho e}{\ln(A) - \ln(A - \tilde{A})}.$$

It is known that the mechanical impedance of the fingertip varies with the pressing force [36], [40]. To measure the variation of M with this force, the plate was supported by two load cells (HBM S2M), as depicted in Fig. 10. Focusing was achieved with the same parameter values as in the previous experiments and repeated at a rate of 500 Hz. The free and loaded displacements of the plate, A and \tilde{A} , were measured at the focus point and sampled at $f_s = 250$ kHz and the maximum displacement was memorized at each focusing period. The finger pressing force, F , was simultaneously recorded. We thus obtained the peak displacement value for each impulse, at a rate of 500 Hz.

B. Results and discussion

The index finger was voluntarily pushed onto the plate and released four times in 16 seconds with a force ranging from zero to approximately one Newton, thus covering the range of forces typically deployed during tactile interaction [41]. The force and the peak displacement amplitudes are plotted in Fig. 11 (top panel) as a function of time. When the applied force was zero, the displacement was about 7 μm . Displacements predictably reduced to about 3 μm when the applied force reached about one Newton. A hysteric behavior being a hallmark of biological tissues, the fingertip impedance can be expected to depend on whether the load increases or decreases [37], [42]. This behavior is quite visible in Fig.11 (bottom left). The value of M was in-line with previously reported values (70 mg to 230 mg) although these values were determined during transverse stimulation [40]. Plate displacement depends non-linearly on the finger normal force 11 (bottom panel, left). The equivalent fingertip mass (bottom panel, right), calculated from the plate displacements, varies between 0 and 100 mg. The behavior and the estimate agree well with the results in [40].

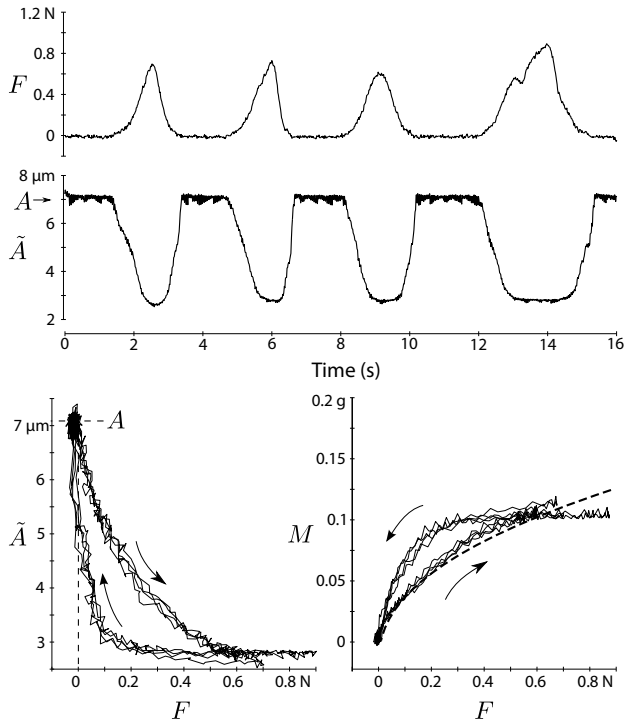


Fig. 11. Finger force and corresponding plate displacement measured at focus times (top panel). (dashed line).

Adopting an expected fingertip mass, $M = 140$ mg for a $F = 1.0$ N pressing force, (7) shows that 70% of the amplitude at focus point is preserved for a product $R_s^2 \rho e$ equal to 66 mg. Considering a glass plate of density $\rho = 2510$ $\text{kg}\cdot\text{m}^{-2}$ and a resolution $R_s = 5$ mm, the corresponding plate thickness is $e = 1$ mm. Fingertip attenuation at the focal point can therefore be easily overcome with a small increase of the plate thickness. Note that according to (6), doubling the plate thickness corresponds to an increase of the energy by a factor 8. This increased thickness would also increase the time constant T_c , see (2), and the resolution, according to (5) and (3). The frequency bandwidth, time reversal duration or number of transducers should therefore have to be adjusted in order to preserve contrast and resolution.

VI. FINGER PULP DISPLACEMENT

In previous work, we have shown that the impulsive displacement produced by the focusing can be easily detected by touch [43]. Detection occurs even though the bandwidth used to achieve impulsive focusing, here from 20 kHz to 70 kHz, is far beyond the range of tactile sensitivity. The stimulation mechanism is therefore not immediate. To understand it, we use the same setup as in Fig. 2 with the difference that the vibrometer laser beam was slightly tilted with respect to the plate normal direction. In this configuration, the beam issued from the specular reflection on the glass plate was scattered away from the objective of the vibrometer. Yet, a portion the beam intensity resulting from a diffuse reflection of the fingertip was sufficient to

enable measurements, provided that the skin were covered with a white film. Figure 12 shows the results.

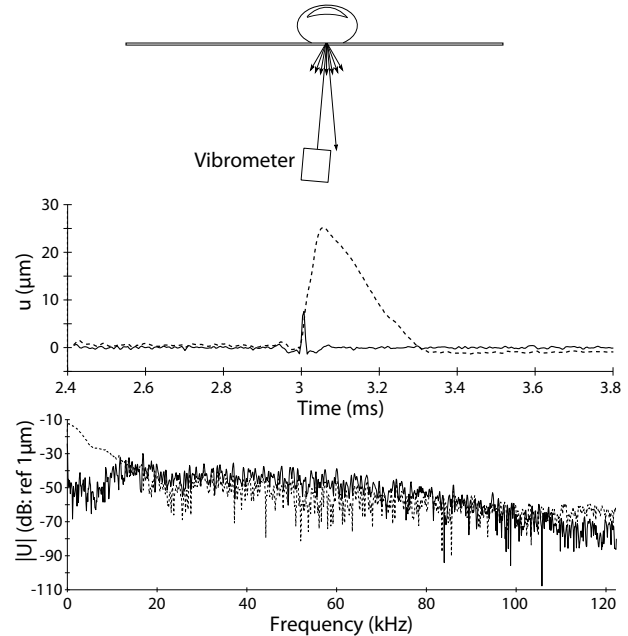


Fig. 12. Laser vibrometer configuration for the measurement of the finger pulp displacement through the glass plate (top). Plate (full line) and fingertip (dotted line) displacements at the focal point (middle panel). Representation in the frequency domain (bottom panel).

The measurements exemplified in Fig. 12 made it evident that before the onset of focusing the plate and the fingertip vibrated in unison, yet at the onset of focusing the plate displacement underwent a peak of 8 μm amplitude for a duration of $R_t \simeq 7$ $\mu\text{s} \simeq 1/(2 \times 70$ kHz) as predicted by (4) while the fingertip skin displacement lasted 0.3 ms and reached a magnitude of 25 μm . It can therefore be concluded that the acceleration at the focal point produced the ejection of the fingertip skin from the plate surface, resulting in a skin displacement much larger in amplitude and duration than the original plate displacement.

Because this phenomenon is essential impulsive and strongly nonlinear, and can be likened to an impact, a drastic spectral transformation should be expected with a transfer of the high frequency energy to the low frequency region. Such transfer is indeed apparent in Fig. 12 (bottom panel) and largely explains why the stimuli are felt strongly and can be easily detected [43], despite the small amplitude of the plate instantaneous displacements.

VII. CONCLUSION

We developed a technique based on the re-focusing of flexural waves, to produce a localized tactile stimulation on a transparent glass plate. The proper design of the physical parameters of a tactile display device based on this technique were established and would also apply, for instance, to the design of a haptically active floor, or to large graphical panels. Key performance factors such as contrast, amplitude, resolution, energy consumption, and achievable refresh rate are all governed by a few key parameters of

dimensional (thickness, area), material properties (Young's modulus, internal dissipation, mass density), and boundary condition (damping attenuation) nature.

The technique was demonstrated using a thin glass plate with 32 lamellar piezoelectric actuators bonded at the periphery and energized by a 1-bit resolution signal. Easily detectable stimuli were achieved with this setup, each of a size smaller than a typical finger contact for an energy expenditure compatible with ordinary portable devices, thus showing the feasibility to provide multitouch tactile stimulation in this context. In other situations where power availability is not so restricted, the technique can be easily scaled up.

While the contact of a finger at the focus point can significantly decrease the peak amplitude reached a focus time, we found that the true stimulation mechanism involved the ejection of the fingertip from the display surface, converting the mechanical energy stored in the form of ultrasonic waves inside the plate into a large, lower frequency displacement of the skin that is strongly felt. A deeper mechanism, that is still speculative at this point, would involve the hardening of the tissues during impulsing loading that would further justify the model approximations. The exact role played by these physics in the perception of the stimulus generated by the technique should be further investigated. For instance, additional insight in this physics could contribute to the reduction (or augmentation) of the residual audible noise emitted but the display despite it being energized in the non-audible range.

APPENDIX A

ATTENUATION VS. REPETITION

Due to natural decay, for $t \geq T$, the displacement amplitude at a point x decreases with a time constant τ . At a time $t \geq T$,

$$u(x, t) = \alpha(t - T)e^{-(t-T)/\tau}, \quad \forall t \geq T.$$

When focusing is repeated with a period T_r , the displacement \hat{u} at a given time t is the superposition of the displacements resulting from all previous focusing, that is,

$$\hat{u}(x, t) = \sum_{r=0}^{\infty} \alpha(t + rT_r - T)e^{-(t+rT_r-T)/\tau}.$$

The contrast ratio is the ratio at focusing time T of the displacement at focus point a divided by the rms displacement at a random position,

$$C = \frac{u(a, T)}{\sqrt{\mathbb{E}[u^2]}},$$

where $\mathbb{E}[u^2] = \frac{1}{S} \int_S u^2(x, t) dx = \frac{1}{T} \int_T u^2(x, t) dt$ owing to the ergodic nature of the wave field inside a bounded propagation medium [44]. Since we seek to determine the impact of attenuation on the repetition rate, we can make the simplifying assumption that the wavefield is a statistically independent and identically distributed (i.i.d.) random process with a null average, that is $\mathbb{E}[\alpha] = 0$, $\mathbb{E}[\alpha(t)\alpha(t' \neq t)] = 0$ and $\mathbb{E}[\alpha^2(t)] = \mathbb{E}[\alpha^2] \neq 0$.

Therefore, the variance of the displacement at a random position, x , after a single occurrence of the focusing process writes $\mathbb{E}[u^2(x, t)] = \mathbb{E}[\alpha^2] e^{-2(t-T)/\tau}$, while after a repetition with a period T_r we have,

$$\begin{aligned} & \mathbb{E}[\hat{u}_{RT}^2(x, t)] \\ &= \mathbb{E}\left[\sum_{r=0}^{\infty} \sum_{s=0}^{\infty} \alpha(t + rT_r - T)\alpha(t + sT_r - T) \dots e^{-(t+rT_r-T)/\tau} e^{-(t+sT_r-T)/\tau}\right] \\ &= \mathbb{E}\left[\sum_{r=0}^{\infty} \alpha^2(t + rT_r - T) e^{-2(t+rT_r-T)/\tau}\right] \\ &= \mathbb{E}[\alpha^2] e^{-2(t-T)/\tau} \sum_{r=0}^{\infty} e^{-2rT_r/\tau} \\ &= \mathbb{E}[\alpha^2] e^{-2(t-T)/\tau} \frac{1}{1 - e^{-2T_r/\tau}}. \end{aligned}$$

The relationship between the variance of the displacements u and \hat{u} after unique or repeated focusing respectively is thus given by,

$$\mathbb{E}[\hat{u}^2(x, t)] = \frac{\mathbb{E}[u^2(x, t)]}{1 - e^{-2T_r/\tau}}.$$

The contrast \hat{C} in the case of a repeated focusing thus reads,

$$\hat{C} = C\sqrt{1 - e^{-2T_r/\tau}},$$

where C is the contrast in the case of single focusing.

APPENDIX B

ENERGY BALANCE

Following Kirchhof's assumptions, in a thin plate the potential energy, E_p , per unit surface is given by [45, p.37],

$$\begin{aligned} \frac{dE_p}{dS}(x, t) &= \frac{1}{2}D \left[\left(\frac{\partial^2 u}{\partial x^2} \right)^2 + \left(\frac{\partial^2 u}{\partial y^2} \right)^2 \dots \right. \\ & \left. + 2\nu \left(\frac{\partial^2 u}{\partial x^2} \right) \left(\frac{\partial^2 u}{\partial y^2} \right) + 2(1 - \nu) \left(\frac{\partial^2 u}{\partial x \partial y} \right)^2 \right], \quad (8) \end{aligned}$$

where $u(x, t)$ is the plate out-of-plane displacement at position x and time t and $D = Ye^3/[12(1 - \nu^2)]$ is the plate rigidity constant. When displacement is recorded during the impulse response acquisition step, the time reversal process produces a peak displacement at time T . At this time, the displacement is maximum over the plate and the out-of-plane velocity and thus the plate kinetic energy is null. After focusing time, transducers remain passive and the energy within the plate decreases due to attenuation. The total energy transferred from the transducers to the plate is thus given by the plate potential energy at focus time. Considering the following normalization of the plate modal shapes,

$$\frac{1}{S} \iint_S \Phi_n^2(x) dx = 1, \quad \forall n,$$

where $\Phi_n(x)$ is the modal deformation of the n^{th} mode at vector position x , and S is the plate surface. The displacement at focusing time is,

$$u(x, t = T) = \frac{u(a, T)}{N} \sum_{n=1}^N \Phi_n(a) \Phi_n(x),$$

with $u(a, T) = A$ the displacement at the focusing point and time. Due to the orthogonality of modal shapes, the total potential energy is the sum of the energy, E_n , of all individual modes, that is,

$$E = \sum_{n=1}^N E_n.$$

From (8) and the dispersion relation of eq. (5) we obtain,

$$E_n = \frac{1}{2} D k_n^4 S \left(\frac{A}{N} \right)^2 = \frac{1}{2} \rho S \left(\frac{A}{N} \right)^2 \omega_n^2$$

With the approximation $\sum_{n=1}^N n^2 \simeq N^3/3$, $R_s = \lambda/2$, $\omega_n = 2\pi n \Delta f$, where $\Delta f = 1/T_c$ is the average distance between successive modes [28], and taking $\nu = 0.3$, we finally obtain the expression (6).

APPENDIX C FINGER ATTENUATION

A harmonic force, $F(a, \omega)$, applied normally to the plate at a point, a , causes a displacement, $U_F(a, \omega)$, such that, $F(a, \omega) = j\omega Z_s(a, \omega) U_F(a, \omega)$, where $Z_p(a, \omega)$ is the plate impedance at point a . During wave focusing, if $Z_l(\omega)$ is additional impedance due to the finger, then, the loaded displacement, relative to the free displacement is,

$$\frac{\tilde{U}(a, \omega)}{U(a, \omega)} = \frac{Z_p}{Z_p + Z_l}.$$

Considering a plate of infinite extent, which amounts to neglecting the scattering of waves caused by the finger contact before focusing, the plate impedance is [46, p.221],

$$\begin{aligned} Z_p(a, \omega) &= \frac{F(a, \omega)}{j\omega U_F(a, \omega)} = 8\sqrt{D\rho_s} \\ &= \frac{4}{\sqrt{3}} e^2 \sqrt{\frac{\rho Y}{1 - \nu^2}} \end{aligned}$$

The impedance of an infinite thin plate is thus real and independent of frequency. The impedance of an inertial load is $Z_l(\omega) = j\omega M$. The attenuation function, $W(\omega)$, is therefore,

$$W(\omega) = \frac{\tilde{U}(a, \omega)}{U(a, \omega)} = \frac{8\sqrt{D\rho_s}}{8\sqrt{D\rho_s} + j\omega M}.$$

In the time domain,

$$\begin{aligned} w(t) &= \frac{1}{2\pi} \int_{-\infty}^{\infty} \frac{Z_s}{Z_s + j\omega M} e^{j\omega t} d\omega \\ &= \begin{cases} \omega_c e^{-\omega_c t}, & \text{if } t \geq 0, \\ 0, & \text{otherwise.} \end{cases} \end{aligned}$$

with $\omega_c = Z_s/M = 8\sqrt{D\rho_s}/M$. The loaded displacement $\tilde{u}(a, t)$ is equal to the convolution of the displacement

$u(a, t)$ without external load by the filtering window $w(t)$. To simplify the calculation, we modelled the unloaded displacement at the focal point, $u(a, t)$, by a gate function, centered on the focusing time, $t = T$, and with a duration equal to the temporal resolution $R_t = 1/(2f_{\text{max}})$. The loaded displacement is then,

$$\begin{aligned} \tilde{u}(a, t) &= \int_{-\infty}^{\infty} u(a, \xi) w(t - \xi) d\xi \\ &= \begin{cases} 0, & \text{if } t - T \leq -R_t/2, \\ u(a, T) [1 - e^{(-R_t/2 - t + T)\omega_c}], & \text{if } |t - T| \leq R_t/2, \\ u(a, T) [e^{(-R_t/2 - t + T)\omega_c}], & \text{if } t - T \geq R_t/2, \end{cases} \end{aligned}$$

The maximum displacement with a finger load is thus reached at time $t = T + R_t/2$ and is,

$$\begin{aligned} \tilde{A} &= \max \{ \tilde{u}(a, t) \} \\ &= \tilde{u}(a, T + R_t/2) \\ &= u(a, T) [1 - e^{-R_t\omega_c}] \\ &= A [1 - e^{-R_t\omega_c}]. \end{aligned}$$

ACKNOWLEDGMENTS

The authors would like to thank Valentin Le Guelvout for his valuable contribution to the development of the driving electronics.

REFERENCES

- [1] V. Levesque, L. Oram, K. MacLean, A. Cockburn, N. D. Marchuk, D. Johnson, J. E. Colgate, and M. A. Peshkin, "Enhancing physicality in touch interaction with programmable friction," in *Proceedings of the SIGCHI Conference on Human Factors in Computing Systems*. ACM, 2011, pp. 2481–2490.
- [2] Y. Visell, A. Law, and J. Cooperstock, "Touch is everywhere: Floor surfaces as ambient haptic interfaces," *IEEE Transactions on Haptics*, vol. 2, no. 3, pp. 148–159, Jul. 2009.
- [3] J. Pasquero, J. Luk, V. Levesque, Q. Wang, V. Hayward, and K. MacLean, "Haptically enabled handheld information display with distributed tactile transducer," *IEEE Transactions on Multimedia*, vol. 9, no. 4, pp. 746–753, Jun. 2007.
- [4] E. Mallinckrodt, A. L. Hughes, and W. Sleator, "Perception by the skin of electrically induced vibrations," *Science*, vol. 118, no. 3062, pp. 277–278, 1953.
- [5] R. M. Strong and D. E. Troxel, "An electrotactile display," *Man-Machine Systems, IEEE Transactions on*, vol. 11, no. 1, pp. 72–79, 1970.
- [6] H. Tang and D. Beebe, "A microfabricated electrostatic haptic display for persons with visual impairments," *IEEE Transactions on Rehabilitation Engineering*, vol. 6, no. 3, pp. 241–248, Sep. 1998.
- [7] M. Altinsoy and S. Merchel, "Electrotactile feedback for handheld devices with touch screen and simulation of roughness," *IEEE Transactions on Haptics*, vol. 5, no. 1, pp. 6–13, Jan. 2012.
- [8] R. H. Cook, "An automatic stall prevention control for supersonic fighter aircraft," *Journal of Aircraft*, vol. 2, no. 3, pp. 171–175, 1965.
- [9] J. Reisinger and J. Wild, *Haptische Bedienschnittstellen*. Vieweg, jan 2008.
- [10] T. Watanabe and S. Fukuki, "A method for controlling tactile sensation of surface roughness using ultrasonic vibration," 1995, pp. 1134–1139.
- [11] T. Nara, M. Takasaki, T. Maeda, T. Higuchi, S. Ando, and S. Tachi, "Surface acoustic wave tactile display," *Computer Graphics and Applications, IEEE*, vol. 21, no. 6, pp. 56–63, 2001.

- [12] M. Biet, F. Giraud, and B. Lemaire-Semail, "Squeeze film effect for the design of an ultrasonic tactile plate," *IEEE Transactions on Ultrasonics, Ferroelectrics and Frequency Control*, vol. 54, no. 12, pp. 2678–2688, Dec. 2007.
- [13] E. C. Chubb, J. E. Colgate, and M. A. Peshkin, "ShiverPaD: A glass haptic surface that produces shear force on a bare finger," *IEEE Transactions on Haptics*, vol. 3, no. 3, pp. 189–198, Jul. 2010.
- [14] M. Wiertelwski, D. Leonardis, D. J. Meyer, M. A. Peshkin, and J. E. Colgate, "A high-fidelity surface-haptic device for texture rendering on bare finger," in *Haptics: Neuroscience, Devices, Modeling, and Applications*, ser. Lecture Notes in Computer Science. Springer Berlin Heidelberg, 2014.
- [15] F. Giraud, M. Amberg, and B. Lemaire-Semail, "Merging two tactile stimulation principles: electrovibration and squeeze film effect," in *World Haptics Conference (WHC), 2013*, 2013, pp. 199–203.
- [16] L. R. Gavrilov, G. V. Gersuni, O. B. Ilyinsky, E. M. Tsurinikov, and E. E. Shchekanov, "A study of reception with the use of focused ultrasound. i. effects on the skin and deep receptor structures in man," *Brain Research*, vol. 135, pp. 265–277, 1977.
- [17] T. Iwamoto and H. Shinoda, "Ultrasound tactile display for stress field reproduction-examination of non-vibratory tactile apparent movement," in *Eurohaptics Conference, 2005 and Symposium on Haptic Interfaces for Virtual Environment and Teleoperator Systems, 2005. World Haptics 2005. First Joint*, 2005, pp. 220–228.
- [18] L. R. Gavrilov, "The possibility of generating focal regions of complex configurations in application to the problems of stimulation of human receptor structures by focused ultrasound," *Acoustical Physics*, vol. 54, no. 2, pp. 269–278, Aug. 2008.
- [19] T. Hoshi, M. Takahashi, T. Iwamoto, and H. Shinoda, "Noncontact tactile display based on radiation pressure of airborne ultrasound," *IEEE Transactions on Haptics*, vol. 3, no. 3, pp. 155–165, Jul. 2010.
- [20] T. Carter, S. A. Seah, B. Long, B. Drinkwater, and S. Subramanian, "UltraHaptics: multi-point mid-air haptic feedback for touch surfaces," in *Proceedings of the 26th annual ACM symposium on User interface software and technology*, 2013, pp. 505–514.
- [21] M. Fink, "Time reversal of ultrasonic fields. i. basic principles," *Ultrasonics, Ferroelectrics and Frequency Control, IEEE Transactions on*, vol. 39, no. 5, pp. 555–566, 1992.
- [22] R. G. Sachs, *The Physics of Time Reversal*. University of Chicago Press, Oct. 1987.
- [23] M. Fink and C. Prada, "Acoustic time-reversal mirrors," *Inverse problems*, vol. 17, no. 1, p. R1, 2001.
- [24] G. Chardon, A. Leblanc, and L. Daudet, "Plate impulse response spatial interpolation with sub-Nyquist sampling," *Journal of Sound and Vibration*, vol. 330, no. 23, pp. 5678–5689, Nov. 2011.
- [25] A. Leblanc, A. Lavie, and R. K. Ing, "The method of fundamental solutions for the impulse responses reconstruction in arbitrarily shaped plates," *Acta Acustica united with Acustica*, vol. 97, no. 6, pp. 919–925, Nov. 2011.
- [26] A. Derode, A. Tourin, and M. Fink, "Ultrasonic pulse compression with one-bit time reversal through multiple scattering," *Journal of Applied Physics*, vol. 85, no. 9, p. 6343, 1999.
- [27] C. Draeger, J. Aime, and M. Fink, "One-channel time-reversal in chaotic cavities: Experimental results," *The Journal of the Acoustical Society of America*, vol. 105, p. 618, 1999.
- [28] C. Hudin, J. Lozada, and V. Hayward, "Spatial, temporal, and thermal contributions to focusing contrast by time reversal in a cavity," *Journal of Sound and Vibration*, vol. 333, no. 6, pp. 1818–1832, Mar. 2014.
- [29] G. Ribay, S. Catheline, D. Clorennec, R. K. Ing, N. Queffrin, and M. Fink, "Acoustic impact localization in plates: properties and stability to temperature variation," *IEEE Transactions on Ultrasonics, Ferroelectrics and Frequency Control*, vol. 54, no. 2, pp. 378–385, Feb. 2007.
- [30] R. T. Verrillo, "Vibrotactile thresholds measured at the finger," *Perception & Psychophysics*, vol. 9, no. 4, pp. 329–330, 1971.
- [31] D. Cassereau and M. Fink, "Time reversal of ultrasonic fields. III. theory of the closed time-reversal cavity," *Ultrasonics, Ferroelectrics and Frequency Control, IEEE Transactions on*, vol. 39, no. 5, pp. 579–592, 1992.
- [32] K. F. Graff, *Wave Motion in Elastic Solids*. Courier Dover Publications, 1975.
- [33] E. K. Dimitriadis, C. R. Fuller, and C. A. Rogers, "Piezoelectric actuators for distributed vibration excitation of thin plates," *Journal of Vibration and Acoustics*, vol. 113, pp. 100–107, Jan. 1991.
- [34] A. Carroll and G. Heiser, "An analysis of power consumption in a smartphone," in *USENIX annual technical conference*, 2010, pp. 271–285.
- [35] M. A. Srinivasan, R. J. Gulati, and K. Dandekar, "In vivo compressibility of the human fingertip," *Advances in Bioengineering*, 1992.
- [36] R. Howe and A. Hajian, "Identification of the mechanical impedance at the human finger tip," *Journal of biomechanical engineering*, vol. 119, pp. 109–114, 1997.
- [37] E. R. Serina, C. Mote, and D. Rempel, "Force response of the fingertip pulp to repeated compression-effects of loading rate, loading angle and antropometry," *Journal of biomechanics*, vol. 30, no. 10, pp. 1035–1040, 1997.
- [38] H. Oka and T. Yamamoto, "Dependence of biomechanical impedance upon living body structure," *Medical and Biological Engineering and Computing*, vol. 25, no. 6, pp. 631–637, 1987.
- [39] E. Serina, E. Mockensturm, C. Mote, and D. Rempel, "A structural model of the forced compression of the fingertip pulp," *Journal of biomechanics*, vol. 31, no. 7, pp. 639–646, 1998.
- [40] M. Wiertelwski and V. Hayward, "Mechanical behavior of the fingertip in the range of frequencies and displacements relevant to touch," *Journal of biomechanics*, vol. 45, no. 11, pp. 1869–1874, 2012.
- [41] A. Smith, G. Gosselin, and B. Houde, "Deployment of fingertip forces in tactile exploration," *Experimental Brain Research*, vol. 147, no. 2, pp. 209–218, Nov. 2002.
- [42] J. Wu, R. Dong, W. Smutz, and A. Schopper, "Modeling of time-dependent force response of fingertip to dynamic loading," *Journal of Biomechanics*, vol. 36, no. 3, pp. 383–392, Mar. 2003.
- [43] C. Hudin, J. Lozada, and V. Hayward, "Localized tactile stimulation by time-reversal of flexural waves: Case study with a thin sheet of glass," *Proceedings of the IEEE World Haptics Conference 2013*, 2013.
- [44] C. Draeger and M. Fink, "One-channel time reversal of elastic waves in a chaotic 2d-silicon cavity," *Physical Review Letters*, vol. 79, no. 3, pp. 407–410, Jul. 1997.
- [45] E. Ventsel and T. Krauthammer, *Thin Plates and Shells: Theory, Analysis, and Applications*. CRC Press, 2001.
- [46] P. Morse and K. Ingard, *Theoretical acoustics*. Princeton University Press, 1986.

Charles Hudin Biography text here.

PLACE
PHOTO
HERE

José Lozada Biography text here.

PLACE
PHOTO
HERE



Vincent Hayward Biography text here.